2012

Giant and anisotropic magnetoresistances in p-type Bi-doped Sb 2Te 3 bulk single crystals

Z J. Yue
University of Wollongong, zy709@uowmail.edu.au

Xiaolin Wang
University of Wollongong, xiaolin@uow.edu.au

Y Du
University of Wollongong, ydu@uow.edu.au

S M. Mahboobeh
University Of Wollongong

Frank F. Yun
University of Wollongong, ffy486@uowmail.edu.au

See next page for additional authors

Giant and anisotropic magnetoresistances in *p*-type Bi doped Sb_2Te_3 bulk single crystals

Z. J. YUE, X. L. WANG,[a] Y. Du, S. M. MAHBOOBEH, Frank F. Yun, Z.X. Cheng, and S. X. DOU
Spintronic and Electronic Materials Group, Institute for Superconducting and Electronic Materials, University of Wollongong, NSW 2522, Australia

PACS 72.15.Gd - Galvanomagnetic and other magnetotransport effects
PACS 75.47.De - Giant magnetoresistance
PACS 75.30.Gw - Magnetic anisotropy

Abstract - Antimony telluride (Sb_2Te_3) compounds are well known as excellent thermoelectric materials and have been confirmed as three dimensional topological insulators recently. In this letter, we have investigated the anisotropic magneto-transport properties of *p*-type Bi doped Sb_2Te_3 bulk single crystals over a broad range of temperatures, degrees and magnetic fields. Giant magnetoresistance (MR) of up to 230% was observed, which exhibits quadratic field dependences in low fields and becomes linear at high fields without any trend towards saturation. The giant MR also shows strong anisotropy with anisotropy ratio up to 210% in angle dependent measurements. The giant MR might result from strong inter-valley and intra-valley scattering of holes and the strong anisotropy is attributable to the anisotropy of hole mobility, relaxation time and effective mass in the Fermi surface. The observed giant anisotropic MR could find applications in Sb_2Te_3 based anisotropic magneto-electronic devices.

a) Corresponding author, Email: xiaolin@uow.edu.au

Antimony telluride (Sb_2Te_3) compounds have rhombohedral structures, space group R_{3m} (D^5_{3d}) and are well-known as narrow gap layered semiconductors [1]. In the past few years, Sb_2Te_3 crystals have been intensively studied because of their excellent thermoelectric performances in the vicinity of room temperatures [2, 3]. Doping effects on thermoelectric properties have been studied to maximize the thermoelectric figure of merit, ZT, which is of critical importance for any potential commercial usage of thermoelectric energy conversion. Sb_2Te_3 based semiconductors have been widely applied in thermoelectric energy converters, refrigerators, and thermostats operating near room temperatures. V. A. Kulbachinskii and H. Y. Lv, *et. al.* have investigated the electrical properties and band structure parameters of Se and Bi doped Sb_2Te_3 from the Hall effects, Shubnikov-de Haas effects (SdH), and thermoelectric effects [4, 5, 6, 7]. Many-valley model was applied to estimate several parameters including the shape and orientation of the energy ellipsoids as well as the density of carriers and the relaxation times. The anisotropy of the relaxation times and effective masses of electrons in Fermi surface was also determined by the comparison of the observed galvanomagnetic coefficients with those predicted from De Haas–van Alphen effects (dHvA) experiments.

Recently, Sb_2Te_3 compounds were confirmed as three dimensional topological insulators with robust surface states comprising a single Dirac cone by angle resolved photoemission spectroscopy (ARPES) measurements and band structure calculations [8, 9]. Topological insulators are quantum materials with an insulating bulk state and a topologically protected metallic surface state with spin and momentum helical locking and a Dirac-like band structure [10, 11]. Unique and fascinating electronic properties, such as the quantum spin Hall effects, magnetoelectric effects, magnetic monopoles, and elusive Majorana states, are expected from topological insulators [12, 13]. Topological insulators have great potential applications in spintronics and quantum information processing, as well as magnetoelectric devices with higher energy efficiency [14, 15]. Up to now, the surface states in topological insulators have been mainly investigated by angle-resolved photoemission spectroscopy (ARPES), scanning tunneling microscopy (STM) and theoretical calculations [16]. To understand the thermoelectric and topological insulator properties and to investigate the possibility of device applications, bulk magnetotransport measurements are indispensable. Shubnikov-de Haas and Aharonov–Bohm oscillations have been observed in Bi_2Se_3 and $Bi_{1-x}Sb_x$ topological insulators [17, 18]. And low temperature linear MR (defined as $(MR=R_H-R_0/R_0)*100$) was observed in Bi_2Te_3 crystal flakes and Bi_2Se_3 nanoribbons [19, 20]. However, to the best of our knowledge, the magnetotransport study of Sb_2Te_3 is very limited. Here, we report the angular dependent MR in Bi doped Sb_2Te_3 bulk single crystals over a broad range of temperatures and magnetic fields. Giant MR of up to 230% was observed in Bi doped Sb_2Te_3 bulk. The observed MR exhibits quadratic field dependences in low fields and becomes linear at high fields. The giant MR represents strong anisotropy and twofold oscillations, especially in high magnetic fields and low temperatures. The observed giant anisotropic MR in Bi doped Sb_2Te_3 bulk single crystals could find applications in anisotropic magnetoelectronic devices.

The Sb_2Te_3 single crystals with 9 % Bi doping used for this study were cleaved from bulk crystals with 99.99% purity. Four-probe transport measurements were performed on a rectangular sample with dimensions of $4 \times 3 \times 0.16$ mm^3 between 2.5 and 200 K using a Quantum Design 14 T Physical Properties Measurement System

(PPMS) The resistance was obtained by applying an electric current I (typically 500 μA) through the two outer contacts and monitoring the voltage drop V between the two inner contacts (typical spacing 1 mm), as shown in the inset of Fig. 1. The current I was applied in the plane, and the magnetic field B was applied perpendicular to the current direction. For some selected magnetic field directions, the field dependence of the MR was measured by sweeping B between 0 and 13 T. Rotation of the sample in constant magnetic field B was used to measure the in-plane anisotropic MR. In the Hall effect measurements, the current was also 500 μA and applied in the plane. The field was increased from 0 to 13 T and was applied perpendicular to the plane. The temperature was fixed at 100 K, and the voltage was detected perpendicular to both the current direction and the field direction.

Figure 1 shows the temperature dependence of the resistivity of a Bi doped Sb_2Te_3 crystal measured in both zero and 13 T. It can be seen that the resistivity in both zero field and 13 T decreases with the temperatures ranging from 200 K to 10 K. Such metallic R(T) curves are typical behavior for Bi doped Sb_2Te_3 and result from the hole-type bulk carriers induced by Sb-Te antisite defects [21]. At high temperatures, the main scattering is phonons and defect scattering, while at low temperatures the dominant scattering is carrier scattering. The Hall coefficient R_{Hall}, as presented in the Fig. 1 inset, is positive in magnetic fields up to 13 T. From the Hall measurements, we determined that the bulk carrier density n is about 2×10^{19} cm^{-3}, and the bulk carrier mobility μ is 1900 cm^2/Vs, in agreement with what has been reported for typical p-type Sb_2Te_3 bulks [5].

Figure 2 displays the MR measured at several temperatures in 13 T and θ = 0° (B//C_3). The MR gradually increases as the temperature is decreased. The maximum value of MR in Bi doped Sb_2Te_3 reaches up to 230% in 13 T at 2.5 K. At low magnetic fields, the MR exhibits an almost quadratic field dependence for all the temperatures, which can be fitted by $MR = kB^2$, with k a constant. The parabola-like B dependence of MR is likely due to the Lorentzian deflection of scattering carriers under the perpendicular magnetic field and is a bulk-dominated effect. The hole executes cyclotron orbits, thereby shortening the mean free path, and thus increasing the resistance. The pattern of curves evolves linearly in applied higher magnetic fields, which might result from scattering holes with open orbits. The inset of Figure 2 shows the strong anisotropic MR in the Bi doped Sb_2Te_3 at 2.5 K through the comparison of MR with H//ab and H//C_3 (0° and 90°).

Figure 3(a) shows polar plots of the angular dependence of the MR measured in several magnetic fields at 2.5 K. The magnetic fields, ranging from 4 to 13 T, were kept constant during each rotation. The observed angular dependence of the MR displays strong anisotropy and a twofold symmetry. Wide peaks appear around the perpendicular field configuration (about θ = 15º, 195º) and dips around the parallel field configuration (about θ = 105º, 285º). This suggests that the MR is most strongly pronounced in out-of-plane high fields. In contrast, the MR anisotropy ratio (defined as $(MR_\theta\text{-}MR_{min})/MR_{min}\times100\%$) increases with magnetic fields decreasing and reaches a maximum of 210% in 4 T at 2.5 K, as presented in Fig. 3(b). This suggests that the MR anisotropy ratio is most strongly pronounced in low fields at a fixed temperature. The common feature is that the peaks and dips of the plots are present at the same θ values. Figure 4(a) displays polar plots of the angular dependence of the MR measured at 13 T for various temperatures. The temperatures, ranging from 200 to 2.5 K, were kept constant during each rotation. The observed angular dependence of the MR displays anisotropic features and a twofold symmetry, which is similar to that shown in Fig. 3. Furthermore, both the MR and the MR anisotropy ratio are strongly pronounced at low temperatures.

The well established Kohler's rule suggests that the MR of a material is a universal function of B as a result of the Lorentz force deflection of carriers. At high field, most materials show saturating MR. Therefore, such a giant anisotropic non-saturating MR in our Bi doped Sb_2Te_3 bulk crystals is unusual. Linear quantum-MR theory was originally developed by Abrikosov based on gapless semiconductors and at the extreme quantum limit to explain the observed giant linear MR in doped silver chalcogenides [22]. However, it is difficult to reach the extreme quantum limit in our Bi doped Sb_2Te_3 because of high hole density. Metals that contain Fermi surfaces with open orbitals in some crystallographic directions, including Cu, Ag, Au, Mg, Zn, Sn, Pb and Pt, will also exhibit large no-saturated MR for fields applied in those directions [23]. These MR are positive and linear in high magnetic fields. And, they present obvious anisotropy because of anisotropy of Fermi Surface, which are similar what we observed in p-type topological insulator Sb_2Te_3 [24]. In addition, no-saturated MR can occur in semiconductors as a consequence of strong electrical disorder, which is related to the carrier mobility but independent of carrier density. They are also positive and have transitions from a quadratic field dependence at low fields to a linear dependence at higher fields. And the high-field MR was found to be linear at all temperatures ranges [25].

The giant and high-field linear MR with twofold symmetry of anisotropy in our samples is likely to be related to the configurations of the valence bands. The valence bands of undoped Sb_2Te_3 are multi-valley bands and consist of upper and lower

valence bands. Sb_2Te_3 has a non-spherical Fermi surface consisting of six ellipsoids tilted at an angle to the basal plane, where the two valence bands are responsible for conduction [26]. Both valence bands are filled by holes with different mobilities, effective masses, and concentrations in different valleys. The non-saturating linear MR suggests that holes have open orbits along the Fermi surface, because the MR should saturate at high B if the orbits are closed in high fields [23]. Doping not only increases the density of holes and decreases the mobility of holes, but also increases the additional impurity scattering. The main mechanisms of scattering in Bi doped Sb_2Te_3 are acoustic phonon scattering, impurity scattering, and intravalley and intervalley scattering. The giant MR might come from intravalley and intervalley scattering in the upper valence band and impurity scattering from doping induced impurity bands [24]. Furthermore, the upper and lower valence bands in Sb_2Te_3 are anisotropic, with effective mass anisotropy of about 3.8, due to the anisotropy of the ellipsoidal hole pockets. The hole scattering and the relaxation time are anisotropic due to the anisotropy of the ellipsoidal hole pockets. The giant anisotropic MR might result from the anisotropy of the Fermi surface in *p*-type Bi doped Sb_2Te_3.

In conclusion, we measured angular dependent MR in *p*-type Bi doped Sb_2Te_3 single crystals in different magnetic fields and temperatures. Giant MR and strong anisotropy of MR were observed, especially in high magnetic fields and low temperatures. The giant MR might result from intravalley and intervalley scattering of holes and the strong anisotropy might result from the anisotropic carrier mobility, relaxation time and effective mass in Fermi surface. Based on the observed giant, high field linear MR and strong anisotropy, the Bi doped Sb_2Te_3 single crystals might have potential applications in anisotropic magneto-electronic devices, such as anisotropic magnetic field sensors, operated at low temperatures and high fields.

Acknowledgements

XL Wang thanks the Australian Research Council for supporting this project through a Discovery project.

REFERENCES

1. Kullmann W., Geurts J., Richter W., Lehner N., Rauh H., Steigenberger U., Eichhorn G. and Geick R., *Phys. stat. sol. (b)*, **125** (1984) 131.
2. Thonhauser T., Scheidemantel T. J., Sofo J. O., Badding J. V. and Mahan G. D., *Phys. Rev. B*, **68** (2003) 085201.
3. Kim Y., DiVenere A., Wong G. K. L., Kettersonb J. B., Cho S. and Meyer J. R., *J. Appl. Phys.* **91** (2002) 715.
4. Kulbachinskii V. A., Miura N., Nakagawa H., Arimoto H., Ikaida T., Lostak P. and Drasar C., *Phys. Rev. B*, **59** (1999) 15733.
5. Kulbachinskii V. A., Dashevskii Z. M., Inoue M., Sasaki M., Gao W. X., Lostak P., Horak J. and Visser A. de, *Phys. Rev. B*, **52** (1995) 10915.
6. Lv H. Y., Liu H. J., Pan L., Wen Y. W., Tan X. J., Shi J. and Tang X. F., *Appl. Phys. Lett.*, **96** (2010) 142101.
7. Kulbachinskii V. A., Kaminsky A. Yu, Lunin R. A., Kindo K., Narumi Y., Suga K., Kawasaki S., Sasaki M., Miyajima N., Lostak P. and Hajek P., *Semicond. Sci. Technol.* **17** (2002) 1133.
8. Kong D., Chen Y. L., Cha J. J., Zhang Q. F., Analytis J. G., Lai K. J., Liu Z. K, Hong S. S., Koski K. J., Mo S. K., Hussain Z., Fisher I. R., Shen Z. X. and Cui Y., *Nature Nanotechnology*, **6** (2011) 705.
9. Zhang J. S, Chang C. Z., Zhang Z. C, Wen J., Feng X., Li K., Liu M. H., He K., Wang L. L., Chen X., Xue Q. K., Ma X. C. and Wang Y. Y., *Nature Communications*, **2** (2011) 574.
10. Hasan M. Z. and Kane C. L., *Rev. Mod. Phys.*, **82** (2010) 4.
11. Qi X. L. and Zhang S. C., *Rev. Mod. Phys.*, **83** (2011) 1057.
12. Bernevig B. A., Hughes T. L. and Zhang S. C., *Science*, **314** (2006) 1757.
13. Hsieh D., Qian D., Wray L., Xia Y., Hor Y. S., Cava R. J. and Hasan M. Z., *Nature*, **452** (2008) 970.
14. Moore J. E., *Nature*, **464** (2010) 194.
15. Wang X. L., Dou S. X. and Zhang C., *NPG Asia Mater.*, **2** (2010) 31.
16. Chen Y. L., Analytis J. G., Chu J. H., Liu Z. K., Mo S. K., Qi X. L., Zhang H. J., Lu D. H., Dai X., Fang Z., Zhang S. C., Fisher I. R., Hussain Z. and Shen Z. X., *Science*, **325** (2009) 178.
17. Peng H. L., Lai K. J., Kong D. S., Meister S., Chen Y. L., Qi X. L., Zhang S. C., Shen Z. X. and Cui Y., *Nat. Mater,*. **9** (2010) 225.
18. Taskin A. A. and Ando Y., *Phys. Rev. B*, **80** (2009) 085303.
19. Qu D. X., Hor Y. S., Xiong J., Cava R. J. and Ong N. P., *Science*, **329** (2010) 821.
20. Tang H., Liang D., Qiu R. L. J. and Gao X. P. A., *ACS Nano*, (2011) **5** (9), 7510.
21. Abrikosov A. A., *Phys. Rev. B*, **85** (1998) 2788.
22. Abrikosov A. A., *Phys. Rev. B*, **60** (1999) 4231.
23. Feng D. and Jin G. J., *Introduction to condensed matter physics*, **1**st, (World Scientific Publishing Company, China), (2005) 212
24. Fawcett E., *Adv. Phys.*, **13** (1964) 139.
25. Johnson H. G., Bennett S. P., Barua R., Lewis L. H. and Heiman D., *Phys. Rev. B*, **82** (2010) 085202.
26. Zuev Y. M., Lee J. S., Galloy C., Park H. and Kim P., *Nano Lett.*, **10** (2010) 3037.

FIGURE CAPTIONS

FIG. 1 Resistivity of *p*-type Sb_2Te_3 as a function of temperatures in 0 T and 13 T. The insets show the measurement schematic diagram (left) and Hall resistance as a function of field at 100 K (right).

FIG. 2 MR as a function of magnetic fields for several temperatures from 2.5 K to 200 K. The inset shows a comparison of MR under out-of-plane and in-plane fields of 13 T at 2.5 K.

FIG. 3 Polar plots of (a) angular dependences of MR and (b) anisotropy ratios of MR at 2.5 K in different fields.

FIG. 4 Polar plots of (a) angular dependences of MR and (b) anisotropy ratios of MR in 13 T at different temperatures.

FIGURE

Fig. 1

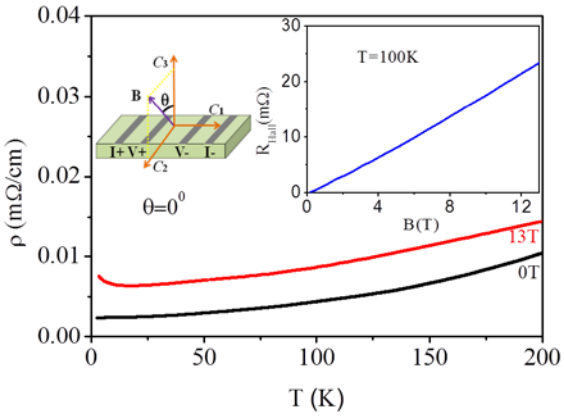

Fig. 2

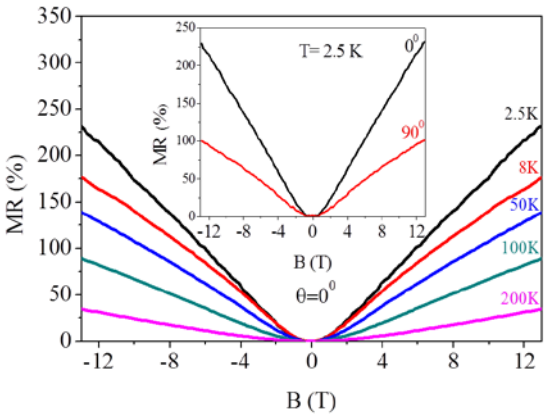

Fig. 3(a)

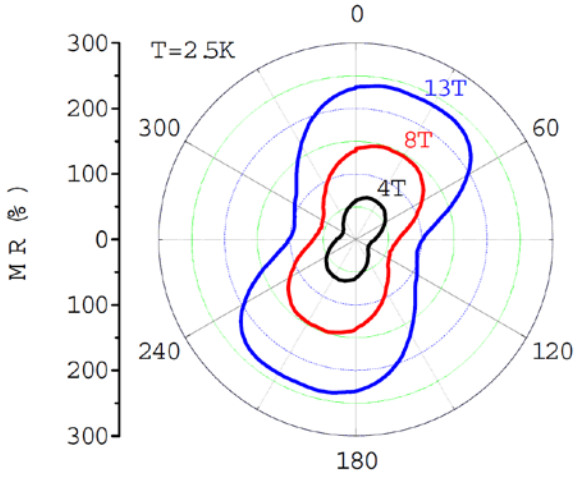

(b)

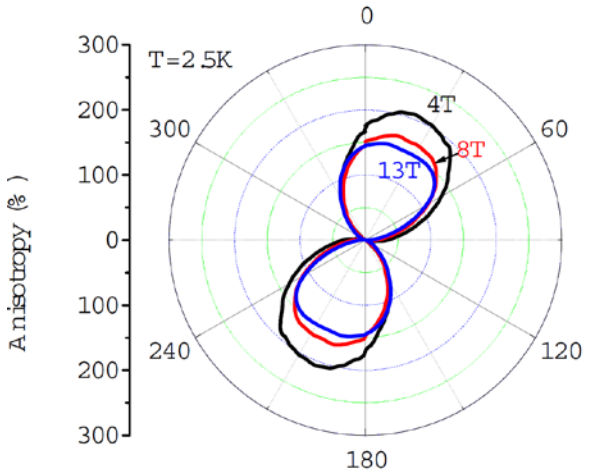

Fig. 4(a)

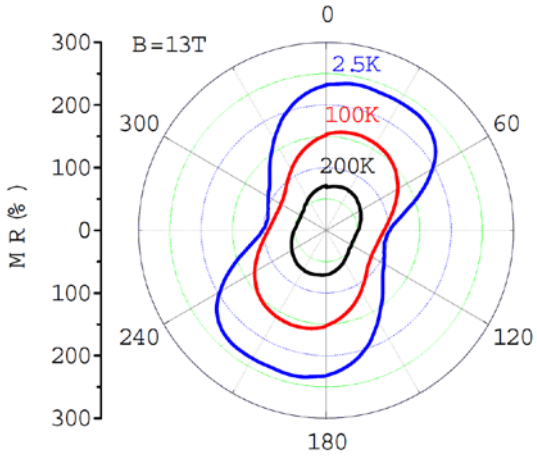

(b)